Scintillation efficiency of binary Li_2O-$2SiO_2$ glass doped with $Ce^{3+}$and Tb^{3+} ions

Y. Tratsiak[1,2], A.Fedorov[2,3], G. Dosovitsky[3], O. Akimova[3], E. Gordienko[3], M. Korjik[2,3], V.Mechinsky[2,3], E. Trusova[2,4]

[1]Research Institute for Physical Chemical Problems of Belarusian State University, Leningradskaya str. 14, 220006 Minsk, Belarus
[2]Research Institute for Nuclear Problems, Bobruiskaya str. 11, 220006 Minsk, Belarus
[3]NRC "Kurchatov Institute", Moscow, Russia
[4] Belarusian State Technological University, Sverdlova str. 13a, 220006 Minsk, Belarus

Highlights

- The photo-luminescence and scintillation properties of binary Li_2O-$2SiO_2$ glasses doped with $Ce^{3+}$and Tb^{3+} were investigated;
- Li_2O-$2SiO_2$ glasses doped with Tb^{3+} showed scintillation light yield up to 31000 ph/MeV.

Abstract

Photo- and radioluminescent properties of lithium silicate glasses doped with $Ce^{3+}$and Tb^{3+}ions were evaluated. Glasses doped with Ce^{3+} ions exhibit a shift of radioluminescence to photo-luminescence band. This effect was explained by a distribution of the crystal field strength in the activator sites, what results in the competition between different types of Ce^{3+} ions in absorbing excitation energy from the matrix and limits a light yield of the Ce^{3+} doped glass. We also investigated the possibility to use Tb^{3+} ion instead of Ce^{3+} as an alternative activator for a glass doping. Spin-orbit interaction plays a major role in the formation of electronic terms in Tb^{3+}, where as an effect of the crystal field is small enough to form a distribution of emitting centers. Tb^{3+}-doped samples demonstrate light yields up to 31000 ph/MeV with the concentration quenching starting at the levels of 10 at %. We also studied the effect of luminescence sensitization of Tb^{3+} ions by Ce^{3+} in the glasses co-doped with Ce^{3+} and Tb^{3+}.

Keywords: glasses, scintillators

Introduction

Ce^{3+}-doped binary oxide glasses and glass ceramics containing metal oxides and silica were found to be suitable matrices for the preparation of scintillating materials [1-3]. They have crystalline structure what allows for additional improvement of the material properties. By introducing fluorine in the ligands and varying the content of metal oxide in the final composition one can obtain luminescent materials with various properties: high light yield of both scintillation and photoluminescence, or quenched scintillation and highly efficient photoluminescence [4]. Among such materials, Ce^{3+}-doped Li_2O-SiO_2 glass [5-8] is one of the most widely used scintillation materials for thermal neutron detection.

Nevertheless, there is a little progress in the improvement of Ce^{3+}-doped glass scintillator light yield due to the combination of several factors. First of all, there is a poor efficiency of transfer of matrix excitations to activating ions. Obviously, it can be improved by increasing the activator content in the glass. Relatively large concentration of Ce^{3+} in the silica glass can be achieved by adding certain components to the starting raw material mixture. For instance, the addition of SiC allows maintaining reducing conditions during the glass formation at high temperatures not only in the inert atmosphere but also in air [9]. However, neither for Li_2O-SiO_2 silicate nor for phosphate glasses [10] a significant increase in the Ce^{3+} content was achieved. The light yield can also be improved by the partial crystallization of the mother glass [1], however, the introduction of additional glass modifying ions, like Mg^{2+}, or glass net creating ions, like Al^{3+}, into the binary system results in the simultaneous formation of several types of crystallites in the glass matrix and not all of them exhibit scintillation properties while still capturing Ce^{3+} ions. Finally, at high Ce^{3+} content a part of Ce^{3+} unavoidably oxidizes into the Ce^{4+} leading to the brownish coloration of the glass. High Ce^{4+} concentration in the glass results in the dramatic decrease of the scintillation light yield [11].

Besides Ce^{3+}, other ions such as Tb^{3+} [12-15] are also considered to be perspective activators for glass-based scintillators. Contrarily to Eu ions, which are hard to stabilize exclusively in either 2+ or 3+ state in the glass due to the strong influence of the glass composition on Eu^{3+}/Eu^{2+} ratio [16,17], Tb^{3+}ions can be easily stabilized in the trivalent state in the glass matrices, regardless of the atmosphere used for their preparation through high-temperature annealing. Tb^{3+} emits luminescence through the number of intra-configurational f-f electronic transitions in the spectral range of 350-650 nm that matches well the spectral sensitivity region of semiconductor photo-receivers [18,19].

In this article, we conducted a comparative study of photo- and radioluminescent properties of Li_2O-$2SiO_2$ glasses doped with Ce^{3+} and/or Tb^{3+}. Tb^{3+}-doped glass was shown to be an efficient material for scintillators exhibiting light yields up to 31000 ph/MeV. In spite that scintillation decay time of Tb^{3+} doped glass is on the order of milliseconds, it makes Li_2O-$2SiO_2$:Tb glass very prospective material for threshold neutron counters with photo-diode readout.

Materials Preparation and Methods

Synthesis

Li_2CO_3, CeO_2, Tb_4O_7 and SiO_2 of 5N analytical grade were used as starting materials. Glasses were prepared by the melt-quenching technique. Li_2CO_3 and SiO_2 were mixed in corresponding proportions and homogenized by milling. Glass was melted in 50 ml corundum

crucibles for 2 h at 1350 °C in FALORNI gas furnace in the reducing atmosphere (CO-rich). The amount of RE oxide in the starting oxide mixture was varied in the range 1-9.5 at. % with respect to Li^+ ions (see Table 1). Molten glasses were cast on the steel surface and then the obtained samples were annealed at 450 °C for 4 h in the muffle furnace to reduce stresses before mechanical processing. Transparent and homogenous glasses were cut and polished to obtain 1 mm thick samples.

Table 1. List of prepared samples

Short name	Glass composition	RE ion concentration (at. % of Li^+ ion)
LiCe	Li_2O-$2SiO_2$	Ce^{3+} (1)
LiTb(*1*)	Li_2O-$2SiO_2$	Tb^{3+} (0.9)
LiTb(*2*)	Li_2O-$2SiO_2$	Tb^{3+} (2.5)
LiTb(*3*)	Li_2O-$2SiO_2$	Tb^{3+} (5.0)
LiTb(*4*)	Li_2O-$2SiO_2$	Tb^{3+} (9.5)
LiTb(*2*), Ce	Li_2O-$2SiO_2$	Tb^{3+} (2.5), Ce^{3+} (2.5)

Obtained samples (LiCe and LiTb(*4*)) and their glowing under UV lamp excitation (312 nm) are in Fig 1.

Fig 1. Polished plates of obtained glass samples and their glowing under UV lamp excitation (312 nm): a - LiTb(*4*), b - LiCe

Measurements

X-ray excited radioluminescence (RL) measurements were carried out using custom made apparatus featuring a CCD detector (Jobin-Yvon Spectrum One 3000) coupled to a monochromator (Jobin-Yvon Triax 180) with 300 or 600 grooves/mm gratings. RL was excited by X-ray irradiation using a Philips 2274 tube operating at 20 kV and 20 mA. X-ray irradiation of the samples was carried out in the same geometry, the exposition time was varied only. All samples at measurements were covered with 1 mm thick aluminum mask with Ø5mm window to

manage similar light collection conditions for the samples having different shape. Thickness of the samples was enough to absorb X-ray irradiation by measured samples and reference BGO sample of the same thickness as well.

Optical absorption spectra were recorded using Varian Cary 50 spectrophotometer in the 190-1100 nm wavelength range.

Steady-state photoluminescence (PL) spectra were measured using a xenon lamp as the excitation source, double monochromator (Jobin-Yvon Gemini 180 with 150 or 600 grooves/mm gratings), and nitrogen-cooled CCD detector coupled to a monochromator (Jobin-Yvon Micro HR). For samples with Tb^{3+} ions the KV418 filter was used to cut off excitation bands of second and higher orders.

Light yield measurement of the slow scintillation

LY measurement in pulse mode and pulse height analysis are suitable with scintillation materials, having scintillation kinetics in the range from nanoseconds to a few tens of microseconds. However, such measurements are hardly performed with any ADCs available for scintillation counting when scintillation kinetics has a time constant in a millisecond range. Therefore, we considered two ways to evaluate LY of Tb^{3+} doped samples.

First, LY can be estimated from the comparison of the integrals under RL spectra. This method allows to compare LY of different samples, if X-rays of excitation are completely absorbed in the sample and conditions for the light collection remains the same for the samples. However, steady state excitation with X-rays does not allow to discriminate scintillation and phosphorescence.

Second, LY can be measured by the method, using PMT in the current mode, which is based on comparison with standard single crystal scintillators with subsequent results corrections on PMT sensitivity at different wavelength regions. This method requires an application of several standard scintillators: when scintillation bands of the sample and reference crystal are very different in spectra, some of the reference crystals are hygroscopic, packed in the metal can, and, can be used only with excitation by gamma-quanta. As a first step, LY of Tb^{3+}-doped samples was measured under alpha-particle excitation (^{241}Am source with the energy of 5.5 MeV and the total activity of 10^4 Bq) with a Philips XP2020 PMT in the current mode relative to Ø20 mm x 2 mm thick YAP:Ce reference single crystal, having light yield of 16,000 photons/MeV under gamma-excitation. To ensure similarity of the measurement conditions, a 0.2 mm thick aluminum diaphragm with 5 mm hole diameter was placed between the source and samples and reference YAP:Ce s crystal as well. In such geometry of measurements the LY of samples and YAP:Ce under alpha-excitation is proportional to the PMT anode current after subtraction of PMT “dark” current measured without alpha-source, and is not dependent from the sample

thickness, because alpha particle path in studied samples and reference YAP:Ce single crystal does not exceed several tens of microns. PMT anode current was integrated over time with time constant 0.1 s, and the voltages at the PMT anode load of 100 kΩ, shunted with a 1 μF capacitor was measured with a digital multimeter for all Tb^{3+}-doped samples and compared with that of reference YAP:Ce. PMT anode quasi-constant voltages did not exceed 1 V in all cases, which had negligible influence on the PMT gain due to voltage reduction between last PMT dynode and anode.

YAP:Ce single crystal exhibits the maximum of the radioluminescence at 350 nm, while Tb^{3+}-doped samples have the maximum of the radioluminescence close to CsI(Tl), 560 nm. Since XP2020 PMT is a typical bilkali PMT, its spectral sensitivity at 560 nm is about 3 times less than that at 350 nm. To make corrections on PMT spectral response, we used 1 x 1 inch CsI(Tl) reference crystal with certified LY of 58,000 ph/MeV. Direct measurement of LY of CsI(Tl) at alpha-excitation is impossible due to aluminum housing, which is used for casing of CsI(Tl) due to its affinity to water. Appropriate correction coefficient was obtained in pulse mode by recording pulse height spectra of YAP:Ce and CsI(Tl) reference samples with the same XP2020 PMT and ^{137}Cs (662 keV) gamma-source at the shaping time constant of 3 μs. To evaluate LY of Tb^{3+}-doped samples under gamma-excitation, ratio of anode currents of Tb^{3+}-doped sample and reference YAP:Ce single crystal was multiplied by 16,000 ph/MeV and, then multiplied by boosting correction coefficient to account difference of CsI(Tl) and YAP:Ce light yields.

It's known that LY under alpha-particle- and gamma-excitation often may differ due to different ionization density and connected shielding and quenching factors. In particular, YAP:Ce single crystals have LY under alpha-particle- excitation 3.8 times smaller than under gamma-excitation with the same energy [20]. We had a possibility to correct our LY data for this factor if necessary. Intercalibration was performed by recording pulse height spectra of ^{137}Cs with reference YAP:Ce single crystal and Ce^{3+}-doped glass sample, with successive comparison of response of the samples in current mode with the same PMT. Ratio of 662 keV total absorption peak position in pulse height spectra was found to be similar to the ratio of the voltages at the PMT anode in current mode. This means, that Ce^{3+}-doped glass sample had the same alpha/beta ratio of 3.8 as YAP:Ce single crystal. Taking in to account that Tb^{3+}-doped glass samples has the same composition and structure as Ce^{3+}-doped one, no additional corrections on the difference of alpha/beta ratios of YAP:Ce and Tb^{3+}-doped glass samples were applied.

It should be also noted, that during all LY measurements PMT "dark" current was measured twice, before alpha-irradiation and immediately after irradiation, in 20-30 seconds after alpha-source removal. In all cases, "dark" current values, measured before and after

irradiation were found to be the same, that means absence of long-term afterglow components in all Tb^{3+}-doped samples. In addition, we have observed scintillation pulses produced by alpha-particles with an oscilloscope at the PMT anode, when anode current was integrated over time with much smaller time constant, ~3 ms. Single scintillation pulses were clearly visible, however, of course, mostly overlapped.

All measurements were made at room temperature (RT).

Results

LiCe glass exhibit wide RL band with the maximum at ~ 385 nm attributable to $5d \rightarrow {}^2F_{5/2,7/2}$ transitions of Ce^{3+} ions (Figure 2a) [4]. In Tb^{3+}-glasses a set of narrow bands peaking at 377, 414, 435, 485, 545, 586 and 621 nm and corresponding to the radiation transitions of Tb^{3+} ions was observed (Fig. 2b) [19]. The emission at wavelengths below 490 nm originates from the $^5D_3$ excited state transition to the various components of ^7F ground term, which is split into the seven levels by spin-orbit interaction. Emission bands above 500 nm are due to the transition from $^5D_4$ to ^7F ground state components. We found that transitions from $^5D_4$ to ^7F ground state dominate in the spectra.

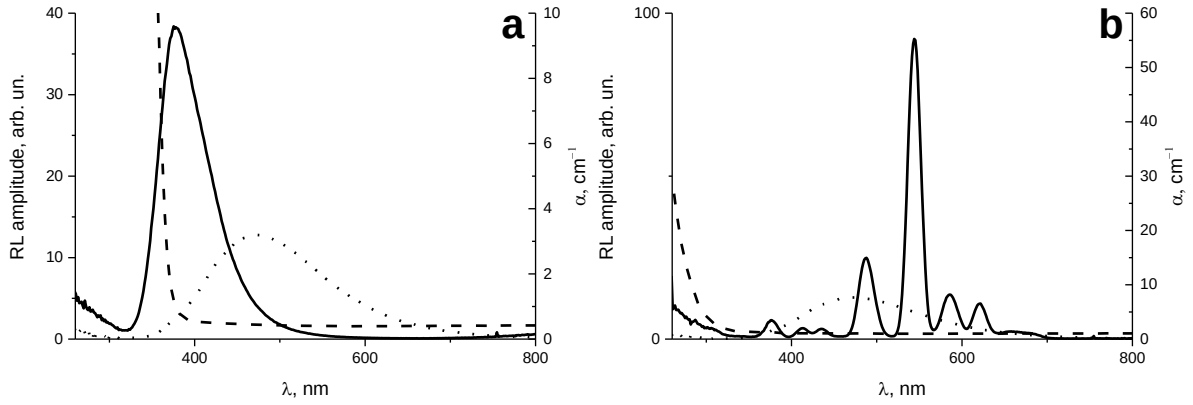

Fig 2. RL spectra of LiCe (a) and LiTb1 (b) samples. Dashed lines correspond to the absorption spectra. Reference spectrum of BGO 2 mm thick sample is presented for a comparison (dotted line)

Similarly to other silicate glasses, Ce^{3+} absorption band peaks near 320 nm, due to the first allowed $4f^15d^0$-$4f^05d^1$ transition [4]. However, due to a strong absorption in the maximum, the excitation spectrum has two artificial maxima at the wavelength corresponding to the edges of the absorption band. PL excitation spectra, luminescence spectra, measured at excitation in a short (300 nm,) and long (350 nm) edge of the band are shown in Fig. 3a-b. In agreement with results obtained for silicate glasses [21] position of emission peaks was found to be dependent on the excitation wavelength (388 and 397 nm for excitation at 300 and 350 nm respectivelly). Figure 3c and 3d show contour plot image demonstrating the dependence of the emission spectra on excitation wavelength. Comparison of the PL and RL spectra shows that PL spectrum is red-

shifted with respect to RL spectrum. It indicates that Ce^{3+}centers emitting at shorter wavelengths more effectively contribute to scintillation.

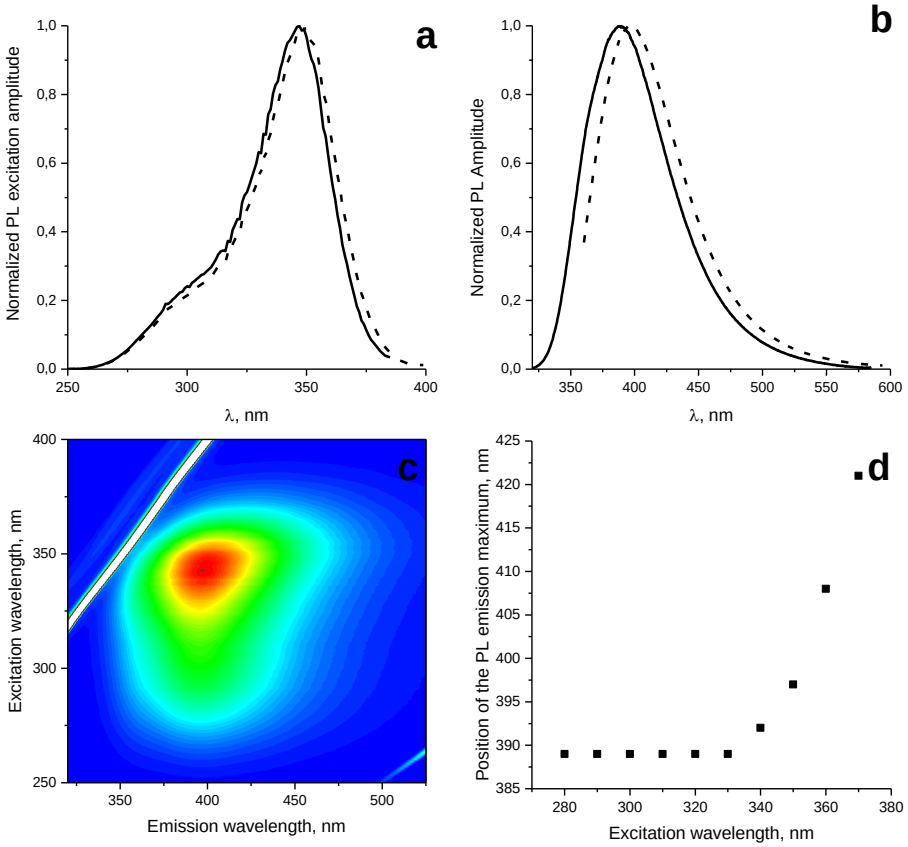

Fig.3. Normalized PL excitation spectra (a) at registration at 418 nm (solid line) and 400 nm (dashed line) and emission spectra at excitation at 300 nm (solid line) and 350 nm (dashed line) for LiCe glass. Contour plot (c, uncorrected) and graph (d) images demonstrating the dependence of the emission spectra on the excitation wavelength.

Unlike in the case of Ce^{3+}-doped samples, we did not observe a significant difference in the spectra of Tb^{3+}-doped samples while scanning excitation wavelength. Figure 4 shows the comparison of PL and RL spectra (4a) and a contour plot image of LiTb (4b) that demonstrates a weak dependence of the emission spectra on the excitation wavelength. It is worth to note that weak Ce^{3+} luminescence upon photoexcitation in LiTb(*2*),Ce sample is observed, whereas it is completely quenched in a radioluminescence. This suggests that Ce^{3+}-ions sensitize the Tb^{3+} luminescence. Similar effect was observed in [22].

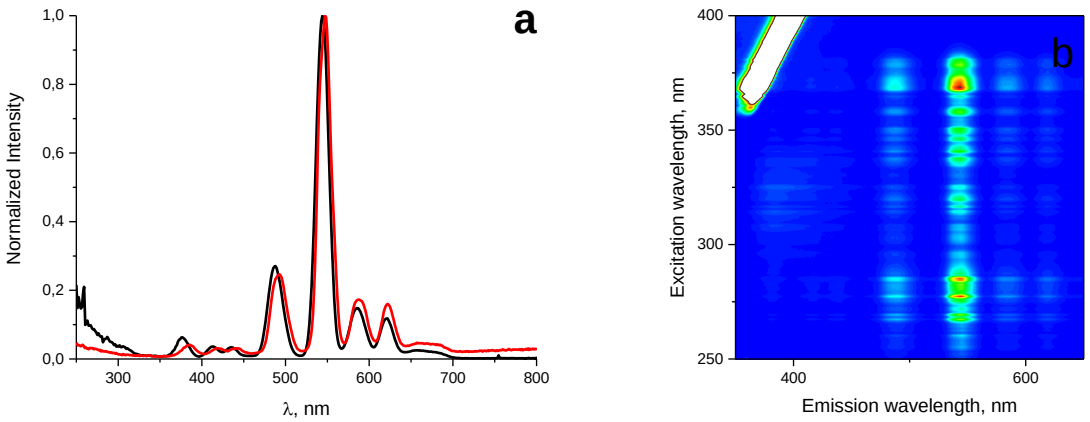

Fig.4. Normalized PL (red) and RL (black) emission spectra at excitation at 277 nm for LiTb glass. Contour plot image (b) demonstrates a low dependence of the emission spectra on excitation wavelength.

Results of the LY evaluation are presented in Table 2.

Table 2. Results of the Light Yield evaluation of different samples

Short name	RE ion concentration (at. % of Li^+ ion)	Light yield measured by PMT in the current mode, ph/MeV
LiCe	Ce^{3+} (1)	6000
LiTb(*1*)	Tb^{3+} (0.9)	8700
LiTb(*2*)	Tb^{3+} (2.5)	19600
LiTb(*3*)	Tb^{3+} (5.0)	27360
LiTb(*4*)	Tb^{3+} (9.5)	31320
LiTb(*2*),Ce	Tb^{3+} (2.5), Ce^{3+} (2.5)	22360

Fig. 5 shows the change of the LY of the LiTb samples versus Tb^{3+} concentration. The LY of LiTb(*2*),Ce is also included in the plot for comparison.

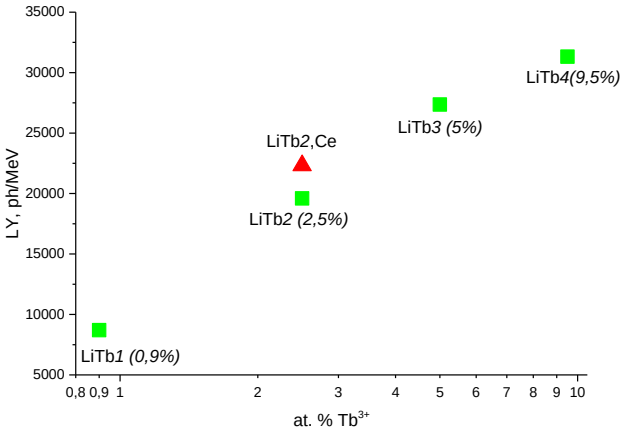

Fig 5. LY of the LiTb samples with different Tb^{3+} concentration in a comparison with LiTb glass co-doped with Ce^{3+} ions

Discussion

In our previous study of the silicate glass doped with low concentration of Ce^{3+}-ions [4] we have shown that the absorption spectrum of the Ce^{3+}-doped glass is characterized by a single wide band with the maximum in the vicinity of 320 nm (31250 cm^{-1}) attributed to electronic transitions from $^2F_{5/2}$ to weakly split $^2D_{5/2,3/2}$ terms. However, the band width (5500 cm^{-1}) is more than two times greater than the split between $^2D_{5/2}$ and $^2D_{3/2}$ states in a free Ce^{3+} ion (2500 cm^{-1}) [1], what is caused by the distribution of the crystalline field in the sites of activator localization. Moreover, the average energy difference between band of configurations of Ce^{3+} ion is 31250 cm^{-1}, what is reasonably smaller that in other oxides [1]. This observation in combination with the indication of a small crystalline field allows suggesting that Ce^{3+} oxy-anionic complex in lithium silicate glass has a loose structure. Cerium ion is likely to be bound to three oxygen ions of surrounding silicon tetrahedra, whereas the crystalline field in the ion localization position is formed by three nearest and other surrounding tetrahedra of the glass net. Disorder of the position of surrounding tetrahedra results in the energy distribution of the lowest (radiating) levels of the Ce^{3+} center. It is confirmed by a systematic shift of the photoluminescence band maxima upon excitation wavelength scanning as seen on Fig. 3. Relatively large energy distribution of the Ce^{3+} radiation states in the glass is fundamentally different to crystalline compounds where this effect is incredibly small. Distribution of states leads to the competition between different groups of Ce^{3+} ions for electronic excitations from the matrix upon its exposure to ionizing radiation. Ce^{3+} ions having larger energy of radiating states are more likely to absorb excitation energy and thus radioluminescence spectrum is shifted to the shorter wavelength range. Distribution of radiating states also explains weak dependence of the radio-luminescence yield on the Ce^{3+} concentration. With an increase of cerium concentration, the activator ions are distributed in a set of groups, therefore, an addition of ions in the groups with radiating levels capable for effective capturing of electronic excitations of the matrix is not increased too much.

The negative effect of the competition between different groups of activating ions is diminished by reducing the influence of crystalline field on the energy levels of activator in the glass. As such alternative solution one can use another activating ion, Tb^{3+}, in which spin-orbit splitting plays a major role in the formation of electronic energy levels. As can be seen from Fig.4 the maxima attributable to f-f transitions practically coincide. As a consequence, Tb^{3+}-doped samples shows increased light yield. Figure 5 shows the influence of the dopant

concentration on the glass LY. Activator concentration is presented in a logarithmic scale. As one can see LY is progressively improved with the increase of the activator concentration. In a situation when distribution of the radiating levels is practically absent, it is more likely that migration of matrix excitations to radiating centers does not play a significant role in the formation of an ensemble of excited Tb^{3+} ions in the glass. As a result, the dominating mechanism is a direct coulomb interaction and consequent capture of carriers. It seems that a concentration quenching occurs at the Tb^{3+} content even larger than 10 at. %. However, silica glass doping with larger amounts of Tb^{3+} ions is limited by some technological difficulties, for example, the need to increase the temperature of the glass preparation. Of note, Ce^{3+} was found to be an efficient sensitizer of Tb^{3+} luminescence in Li_2O-SiO_2 glass: scintillation light yield of samples co-doped with 2.5 at. % of Ce^{3+} increases by 15 %.

Conclusions

We compared luminescent properties of Li_2O-$2SiO_2$ glasses doped with Ce^{3+} and Tb^{3+}. Distribution of radiating energy levels of Ce^{3+} activating ions is likely to be the limiting factor for increasing the scintillation light yield in the glass matrices. Such effect can be reduced in the rare-earth doped glass, in which dopant energy levels become less sensitive to the variation of the crystalline field. The light yield of Li_2O-$2SiO_2$ glasses doped with 9.5 at. % of Tb^{3+} was fond to be at the level of 31000 ph/MeV. Ce^{3+} ions introduced into Tb^{3+}-doped glass act as sensitizers and increase the light yield for up to 15%.

Acknowledgements

The collaboration and research were supported by the H2020 RISE Intelum Project (Grant Agreement 644260), and support of the grant № 14.W03.31.0004 of Ministry of Science and Education of Russian Federation also is appreciated. Authors have many thanks to our colleagues Prof. A.Vedda, Dr. M. Fasoli and Dr. F. Moretti from Department of Materials Science, University of Milano-Bicocca for fruitful cooperation.

This article is dedicated to the memory of Dr. Marvin J. Weber, the pioneer of many novel aspects of the spectroscopy of scintillation materials.

References

1. P.Lecoq, A.Gektin, M.Korzhik, Inorganic scintillators for detecting Systems / Springer, 2017, P.408

2. Chen, G., Yang, Y., Zhao, D., Xia, F., Baccaro, S., Cecilia, A. and Nikl, M. (2005), Composition Effects on Optical Properties of Tb^{3+}-Doped Heavy Germanate Glasses. Journal of the American Ceramic Society, 88: 293–296. doi:10.1111/j.1551-2916.2005.00075.x
3. A.R. Spowart, Neutron scintillating glasses: Part 1: Activation by external charged particles and thermal neutrons, In Nuclear Instruments and Methods, Volume 135, Issue 3, 1976, Pages 441-453, ISSN 0029-554X, https://doi.org/10.1016/0029-554X(76)90057-4.
4. Y. Tratsiak, E. Trusova, G. Dosovitsky, M. Fasoli, M. Korjik, F. Moretti, A. Vedda Photo- and radio-luminescence properties of $3CaO\text{-}2SiO_2$ and $3CaF_2\text{-}2SiO_2$ glasses doped by Ce^{3+} ions / Journal of Luminescence, 2017, 188, P. 289–294
5. V. Khabashesky, M. Vasiliev Demand for new instrumentation for well logging and natural formations monitoring / Proceedings of International Conference "Engineering of scintillation materials and radiation technologies ISMART2016", to be published by Springer, 2017
6. Spowart AR Neutron scintillating glasses: part I. Activation by external charged particles and thermal neutrons / Nucl Instr Meth Phys Res, 1976, 135, P.441-453
7. Spowart AR Neutron scintillating glasses: part II. The effect of temperature on pulse height and conductivity / Nucl Instr Meth Phys Res, 1977, 140, P. 19-28
8. Spowart AR Neutron scintillating glasses: part III. Pulse decay time measurements at room temperature / Nucl Instr Meth Phys Res, 1978, 150, P. 159-163
9. Method for producing luminescent silicate glasses and composites, Patent RU 2564037
10. John S. Neal, Lynn A. Boatner, Dariusz Wisniewski, Joanne O. Ramey New rare-earth-doped phosphate glass scintillators / Proc. SPIE 6706, Hard X-Ray and Gamma-Ray Detector Physics IX, P. 670618. doi:10.1117/12.734561
11. M. Fasoli, A. Vedda, A. Lauria, F. Moretti, E. Rizzelli, N. Chiodini, F. Meinardi, M. Nikl, Effect of reducing sintering atmosphere on Ce-doped sol–gel silica glasses, In Journal of Non-Crystalline Solids, Volume 355, Issues 18–21, 2009, Pages 1140-1144, ISSN 0022-3093, https://doi.org/10.1016/j.jnoncrysol.2009.01.043.
12. Pan Z, James K, Cui Y, Burger A, Cherepy N, Payne S, Mu R, Morgan S Terbium-doped lithium-lanthanum-aluminosilicate oxyfluoride scintillating glass and glass-ceramics / Nucl Instr Meth Phys Res, 2015, A594, P. 215-219
13. W. Chewpraditkul, Q. Sheng, D.Chen, M. Nikl Luminescence of Tb^{3+}-doped oxide glasses with high Gd_2O_3concentration under UV and X-ray excitation / Physica status solidi (a), 2012, 209, P.2578-2582
14. Dongbing He, Chunlei Yu, Jimeng Cheng, Shunguang Li, Lili Hu, Effect of Tb^{3+} concentration and sensitization of Ce^{3+} on luminescence properties of terbium doped

phosphate scintillating glass, In Journal of Alloys and Compounds, Volume 509, Issue 5, 2011, Pages 1906-1909, ISSN 0925-8388, https://doi.org/10.1016/j.jallcom.2010.10.085.

15. M. Zhuravleva, K. Yang, M. Spurrier-Koschan, P. Szupryczynski, A. Yoshikawa, C.L. Melcher, Crystal growth and characterization of LuAG:Ce:Tb scintillator, In Journal of Crystal Growth, Volume 312, Issue 8, 2010, Pages 1244-1248, ISSN 0022-0248, https://doi.org/10.1016/j.jcrysgro.2009.11.021.
16. Liu, S., Zhao, G., Ruan, W., Yao, Z., Xie, T., Jin, J., Ying, H., Wang, J. and Han, G. (2008), Reduction of Eu^{3+} to Eu^{2+} in Aluminoborosilicate Glasses Prepared in Air. Journal of the American Ceramic Society, 91: 2740–2742. doi:10.1111/j.1551-2916.2008.02496.x
17. Yanlin Huang, Kiwan Jang, Xigang Wang, Chuanfang Jiang, Optical properties of Eu^{2+}-doped strontium borate glasses containing F^{-} and Li^{+} ions, In Journal of Rare Earths, Volume 26, Issue 4, 2008, Pages 490-494, ISSN 1002-0721, https://doi.org/10.1016/S1002-0721(08)60124-6.
18. Xianping Fan, Minquan Wang, Guohong Xiong, Spectroscopic studies of rare earth ions in silica glasses prepared by the sol-gel process, In Materials Letters, Volume 27, Issues 4–5, 1996, Pages 177-181, ISSN 0167-577X, https://doi.org/10.1016/0167-577X(95)00279-0.
19. T. Hayakawa, N. Kamata, K. Yamada, Visible emission characteristics in Tb^{3+}-doped fluorescent glasses under selective excitation, In Journal of Luminescence, Volume 68, Issues 2–4, 1996, Pages 179-186, ISSN 0022-2313, https://doi.org/10.1016/0022-2313(96)00022-1.
20. VG Baryshevsky, MV Korzhik, VI Moroz et.al. $YAlO_3$: Ce-fast-acting scintillators for detection of ionizing radiation/NIM B, 1991, 58(2), pp. 292-293
21. V.I. Arbuzov, Bonch-Bruevich V. A. Galant E. I., Przhevuskij A.K. Tolstoy M.N. Inhomogeneous structure of spectra for Eu^{2+} and Ce^{3+} ions in quartz glass / Physics and Chemistry of Glasses, 1982, 8(2). P. (In Russian)
22. Cheng-gang Zuo, An-xian Lu, Li-gang Zhu Luminescence of Ce^{3+}/Tb^{3+} ions in lithium–barium–aluminosilicate oxyfluoride glasses / Materials Science and Engineering: B, 2010, 175(3), P.229–232